

## Assessment of direct glycerol alkaline fuel cell based on Au/C catalyst and microporous membrane

Sarayut Yongprapat<sup>\*1</sup>, Apichai Therdthianwong<sup>1</sup> and Supaporn Therdthianwong<sup>2</sup>

<sup>1</sup>Fuel Cells and Hydrogen Research and Engineering Center, CES, Pilot Plant and Development Training Center, King Mongkut's University of Technology Thonburi (KMUTT), Bang Mod, Thung Khru, Bangkok, 10140 Thailand

<sup>2</sup>Department of Chemical Engineering, Faculty of Engineering, King Mongkut's University of Technology Thonburi (KMUTT), Bang Mod, Thung Khru, Bangkok, 10140 Thailand

(Received September 24, 2013, Revised December 28, 2013, Accepted January 11, 2014)

**Abstract.** The use of a microporous membrane along with Au/C catalyst for direct glycerol alkaline fuel cell was investigated. In comparison with Nafion 112, the microporous Celgard 3401 membrane provides a better cell performance due to the lower ionic resistance as confirmed by impedance spectra. The single cell using Au/C as anode catalyst prepared by using PVA protection techniques provided a higher maximum power density than the single cell with commercial PtRu/C at 18.65 mW cm<sup>-2</sup>. The short-term current decay studies show a better stability of Au/C single cell. The higher activity of Au/C over PtRu/C was owing to the lower activation loss of Au/C. The magnitude of current decay indicates a low problem of glycerol crossover from anode to cathode side. The similar performance of single cell with and without humidification at cathode points out an adequate transport of water through the microporous membrane.

**Keywords:** direct alcohol fuel cell; Au/C; microporous membrane; glycerol; alkaline

---

### 1. Introduction

The electrode reactions of a fuel cell in an alkaline are different from those in an acid environment. This makes a number of catalyst materials to be chosen from for both anode and cathode. The metals such as Pd (Pattabiramen 1997, Shen and Xu 2007) and Au (Betowska-brzezinska 1997, Change *et al.* 1991 and Zhange *et al.* 2012) show much improved catalytic activity toward alcohol electrooxidation in alkaline than in acid. The complete reduction of oxygen is also achieved on various materials such as Pd (Banazawa *et al.* 2009 and Yang *et al.* 1995), Ag (Blizanac *et al.* 2007 and Demarconnay *et al.* 2004) and MnO<sub>2</sub> (Lima *et al.* 2006). With these advantages, a more reaction selective catalyst can be used for both electrodes. The uses of catalyst with low activity towards alcohol electrooxidation as cathode catalyst can help relieve a crossover problem.

There are several required functions of the membrane: preventing mixing of fuel and oxidant, transporting ions between electrodes and providing electrical resistance. To relieve the crossover problem, the use of porous membranes without transport selectivity is possible. All the chemical

---

\*Corresponding author, E-mail: Sarayut.yon@kmutt.ac.th

species can be transported through pore and the membrane also offers the electrical resistance.

The anion-exchange membranes (AEMs) have been developed for alkaline type fuel cells. It normally utilizes quaternary alkylammonium functional groups to offer the anionic conductivity. Despite its decent ion conductivity, the stability of this based functional group is still a major challenge. The conductivity of the membrane was deteriorated by the loss of functional group, alkaline degradation and thermal degradation (Arges *et al.* 2012, Arges *et al.* 2012, Maurya *et al.* 2013, Nunez and Hickner 2012). Unlike the AEMs, the absence of a specific functional group of a porous membrane makes it less prone to the poisoning problem and degradation. Moreover, the porous membranes are relatively cheap and a variety of types are possible.

Lately, Au-based catalysts receive much attention for alcohol electrooxidation in alkaline type fuel cell (Padayachee *et al.* 2013, Yongprapat *et al.* 2012, Xin *et al.* 2012 and Zhang *et al.* 2012). It shows higher catalytic activity than Pt-based catalysts for electrooxidation of polyhydric alcohols such as ethylene glycol and glycerol in alkaline solution (Yongprapat *et al.* 2012). In this study, we reported the performance of the direct glycerol alkaline fuel cell based on microporous polymer fuel cell using Au/C. The Au/C was synthesized by using polyvinyl alcohol (PVA) protection method. The performance of fuel cell using Au/C anode catalyst under various single cell conditions was tested in comparison with that of PtRu/C.

## 2. Methodology

### 2.1 Catalyst preparation

The detail on the preparation of the Au/C catalyst used in this study was described in our previous work (Yongprapat *et al.* 2012). In brief, the Au sol was prepared by using PVA protection method. The Au precursor was reduced to form Au nanoparticles by NaBH<sub>4</sub> in the presence of PVA. After that, the Au sol was immobilized onto Vulcan XC-72R support to obtain 20 wt% Au/C catalysts.

### 2.2 Catalyst layer and MEA preparation

The catalyst ink was prepared by mixing a required amount of the catalyst with isopropanol and a 5 wt% Nafion solution (Electrochem Inc.) in an ultrasonic bath for at least 30 min. The metal loading of the anode catalyst, Au/C or PtRu/C (E-tek), was at 1 mg cm<sup>-2</sup>. The cathode catalyst for all cells was Pt/C (E-tek) loaded at 2 mg cm<sup>-2</sup>. The well-mixed catalyst ink was painted onto a 5 cm<sup>2</sup> commercial gas diffusion layer (GDL) (ELAT, E-tek). The painted electrode was dried in a vacuum oven at 70 °C for 30 min.

Two types of membrane namely Celgard 3401 membrane (Celgard Inc.) a microporous membrane and Nafion 112 membrane (Dupond) were used as membrane electrolyte. Celgard 3401 membrane was soaked in 2 M KOH solution for 30 min and then dried in ambient air. Nafion 112 membrane was pretreated by boiled at 70 °C in sequence of solutions which are de-ionized water, 3 wt% H<sub>2</sub>O<sub>2</sub> and de-ionized water for 30 min each. The MEAs were fabricated by sandwiching the membrane with the anode and cathode gas diffusion electrodes (GDE). The MEA was then clamped both sides by bipolar plates and current collector end-plates (Electrochem Inc.) and tighten at torque of 30 in lb to form a single cell.

### 2.3 Operation of single cell in fuel cell apparatus

A single cell with approximately  $5 \text{ cm}^2$  was used in this study. The anode was fed by a fuel mixture of glycerol and KOH solution at  $1 \text{ ml min}^{-1}$ . Pure oxygen with or without humidification was fed at the cathode at a flow rate of  $46 \text{ ml min}^{-1}$ . The single cell was activated by the fuel and  $\text{O}_2$  for 30 min prior to the performance evaluation. The polarization curves were measured via N3306A electronic load (Agilent). The data were recorded at a current density higher than  $10 \text{ mA cm}^{-2}$  due to the limitation of the electronic load. The electrochemical impedance spectra were measured using PGSTAT 302N (Autolab) with NOVA program. Impedance spectra were obtained at a constant current density of  $50 \text{ mA cm}^{-2}$  in a frequency range between 5 kHz and 0.05 Hz with 10 points per decade, at the amplitude lower

## 3 Results and discussion

### 3.1 The comparison between Celgard 3401 and Nafion 112 membrane

The suitability of single cell using porous membrane was compared with Nafion 112. The MEA was fabricated using PtRu/C as an anode catalyst. The performance of two MEAs with different membrane namely Nafion 112 and Celgard 3401 are compared as shown in Fig. 1. The current density of the fuel cell based on Celgard yielded higher current density than that of Nafion at both temperatures. At  $70 \text{ }^\circ\text{C}$ , the current density at  $0.4 \text{ V}$  and the maximum power density of the single cell with Celgard membrane was  $33.2 \text{ mA cm}^{-2}$  and  $13.36 \text{ mW cm}^{-2}$ , which are around 32% higher than those of the single cell using Nafion at  $25.1 \text{ mA cm}^{-2}$  and  $10.04 \text{ mW cm}^{-2}$ .

The high frequency impedance was used to observe the Ohmic resistance of the single cell. From the impedance spectra in Fig. 2, the Ohmic resistance of the single cell using Celgard shows much lower Ohmic resistance than the single cell with Nafion as can be determined from the x-intercept at the beginning of the spectra. The overall Ohmic resistance of the cell with Celgard

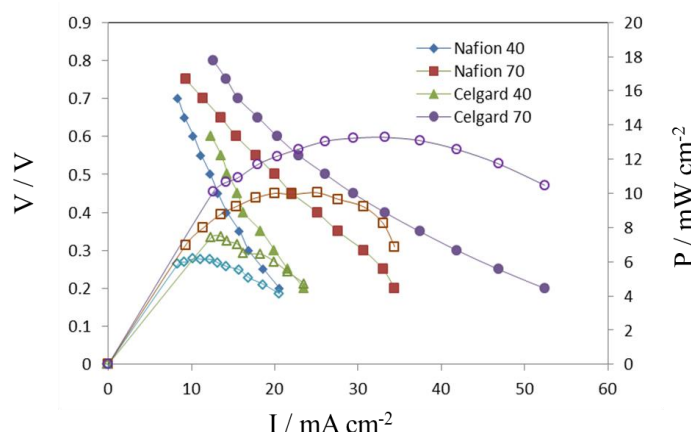


Fig. 1 Polarization curves and power density curves of the single cell using Nafion 112 or Celgard 3401 as a membrane. Fuel feed is a solution of 1 M glycerol and 2 M KOH. The name of each curve defines the type of membrane used and the operating temperature

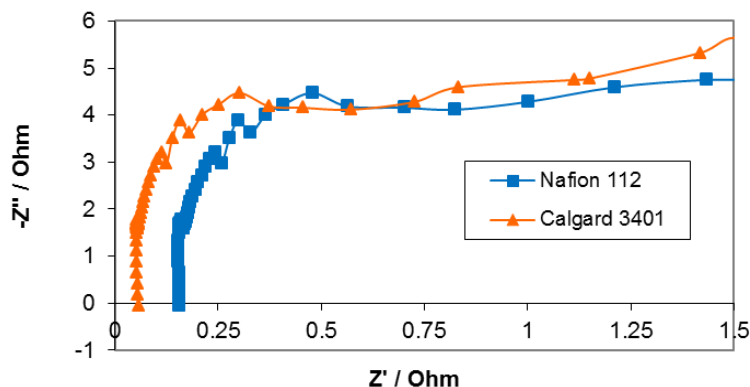


Fig. 2 The high frequency impedance spectra of the single cell using Nafion 112 and Celgard 3401 membranes at a constant current density of 50 mA. Cell was operated at 70 °C, anode feed: 1 ml min<sup>-1</sup> of 1 M glycerol and 2 M KOH, cathode feed: O<sub>2</sub> at 46 ml min<sup>-1</sup>

Table 1 Current density in mA cm<sup>-2</sup> unit and the decay rate from the 1<sup>st</sup> minute and 30<sup>th</sup> minute of the single cell in Fig. 1 at 0.4 V

Membrane	Tcell ( °C)	I at 1 <sup>st</sup> min	I at 30 <sup>th</sup> min	Current decay (%)
Nafion 112	40	16	14.2	11.25
	70	27.2	24.8	8.82
Celgard 3401	40	17.4	16.2	6.90
	70	35	31.2	10.86

was at 0.063 Ohm which is more than 2-fold lower than that of the cell with Nafion at 0.156 Ohm. Since the cell components were similar except for the membrane, the main difference in the overall cell resistance can be referred to the ionic resistance of the membrane. Even though the thickness of Celgard 3401 was only half of that of Nafion 112, the more than 2-fold lower Ohmic resistance of the single cell using Celgard than that of the cell Nafion implied a better ionic conductivity of the Celgard over Nafion.

To complete the fuel cell circuit in this studied system, either OH<sup>-</sup> must be transported from the cathode to the anode or K<sup>+</sup> must be transported from the anode to the cathode. For Celgard, both OH<sup>-</sup> and K<sup>+</sup> should be freely moving between electrodes depending on the diffusion and osmotic condition of the cell since the membrane is not selective. For Nafion, even though it was designed as the cation exchange membrane, the main conducted ion in the alkaline environment becomes OH<sup>-</sup> with part of cation conducted especially in thin membrane such as Nafion 112 (An *et al.* 2012). The overall ionic conduction of Nafion was lowered by the repulsion of the functional group and hydroxide ion. As a consequence, the porous membrane without selective conduction is more capable for the mixed OH<sup>-</sup> and K<sup>+</sup> condition than the cation exchange membrane.

Fig. 3 shows the results of short-term stability test at 0.4 V of both single cells. The stability was calculated by means of decay rate as depicted in Table 1. The current was high in the first minute after current interrupt. The current became quite steady with a small decay after 1 minute. The current density obtained after the first minute, as shown in Table 1, was close to those from

the polarization curve.

The decay rate of both single cells was in the same order of magnitude with a slightly higher current decay of the single cell with Celgard at 70 °C. The glycerol crossover was one of the main concerns of the use of microporous membrane owing to the type of cathode catalyst used in the present study. Pt/C was active for glycerol electrooxidation, and then the glycerol crossover should deteriorate the activity of Pt/C and single cell. However, the slightly different decay rate of both cells indicates that the glycerol crossover through the porous membrane was not much serious. In addition, the decay rate of around 10% was close to that of the decay of anode catalyst alone (Yongprapat *et al.* 2012).

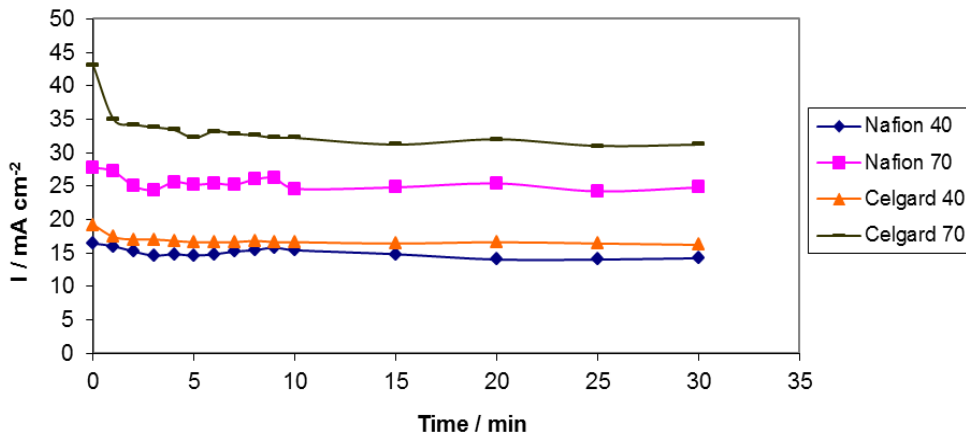


Fig. 3 The current density decay of the single cell in Fig. 1 at 0.4 V

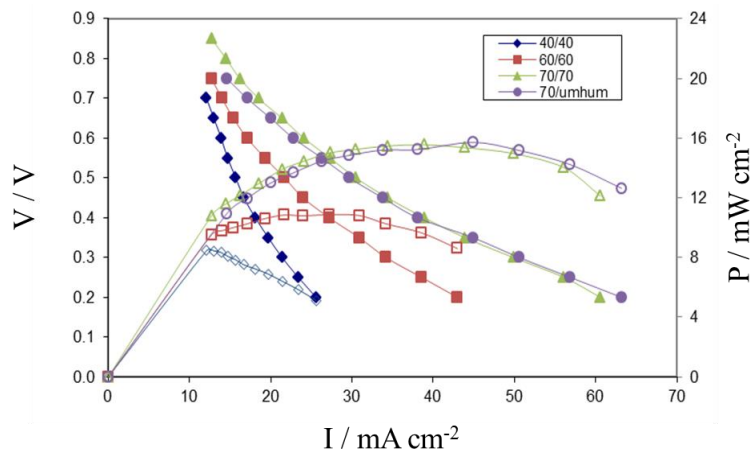


Fig. 4 Polarization curves and power density curves of the single cell using Au/C as an anode catalyst. Fuel feed is a solution of 1 M glycerol and 2 M KOH. The name of each curve defines the cell temperature and humidification temperature; 40/40 means cell temperature is 40 °C and humidification temperature at 40 °C

### 3.2 Performance of fuel cell using Au/C catalyst

The Au/C catalyst used was well-dispersed Au nanoparticles on Vulcan XC-72R with average size of 3.81 nm (Yongprapat *et al.* 2012). Fig. 4 shows the polarization and power density curves of the single cell contained the prepared Au/C catalyst at different cell temperatures and humidification conditions. The performance of the cell substantially depended on the cell temperature. The current density at 0.4 V was greatly improved from 18.1 mA cm<sup>-2</sup> at 40 °C to 27.2 and 38.9 mA cm<sup>-2</sup> at 60 and 70 °C, respectively. The highest power density at 70 °C was 15.82 mW cm<sup>-2</sup> at 0.35V. The current density increasing rate higher than one fold can be expected since the electrooxidation of glycerol on Au-based catalysts involves the C-C bond breaking. The main electrooxidation products were the C<sub>1</sub> and C<sub>2</sub> molecules (Yongprapat *et al.* 2012).

The humidification condition at the cathode showed no effect on the cell performance. The polarization curve of the cell operated at 70 °C humidification temperature was overlay on that of the cell without humidification. Unlike in acid environment, water was one of the reactants of the cathode reaction of alkaline type fuel cells



In the PV loops of the two infarct models without hydrogel injectate (Fig. 2(a)), a clear shift to the right of the ESPVR curves compared to the healthy reference case is observed. This rightward shift is largest for the SDI model. For the EDPVR, a similar rightward shift is seen for the SDI case while no difference is observed between the ischemic infarct (II) case and the healthy (H) case. With regard to the cardiac function, a decrease in contractility  $E_{ES}$  of 19% and 54% relative to the healthy reference is shown for models II and SDI. An increase in  $V_0$  by 63% and 183%, a reduction of SV of 70% and 39%, and a drop in EF of 71% and 67% are seen for II and SDI cases, respectively, in comparison to the healthy control case (Table 2).

Inadequate amount of water should limit the cell performance. Without cathode humidification, water must be transported from the anode. Thus, transportation of the water was one of the crucial properties of the membrane.

The overlay of polarization curves here indicated a sufficient water transport through the pore of the membrane. For a reference, the Celgard 3401 used in this study has 41% porosity with 25 μm thickness. The thin and high porosity of this membrane ensure the water crossover.

Fig. 5 shows a short-term current density decaying at a constant voltage of 0.4 V and various cell operating conditions. As time passes, the current density was slowly declined with a small variation. The current density was quite constant at low temperature but dropped faster at an

Table 2 Current density in mA cm<sup>-2</sup> unit and the decay rate from the 1<sup>st</sup> minute and 30<sup>th</sup> minute of the single cell in Fig. 4 at 0.4 V

T <sub>cell</sub> /T <sub>hum</sub> ( °C)	I at 1 <sup>st</sup> min	I at 30 <sup>th</sup> min	Current decay rate (%)
40/40	19.8	18.6	6.06
60/60	32.8	30.0	8.54
70/70	41.6	36.0	13.46
70/unhum	41.0	37.2	9.27

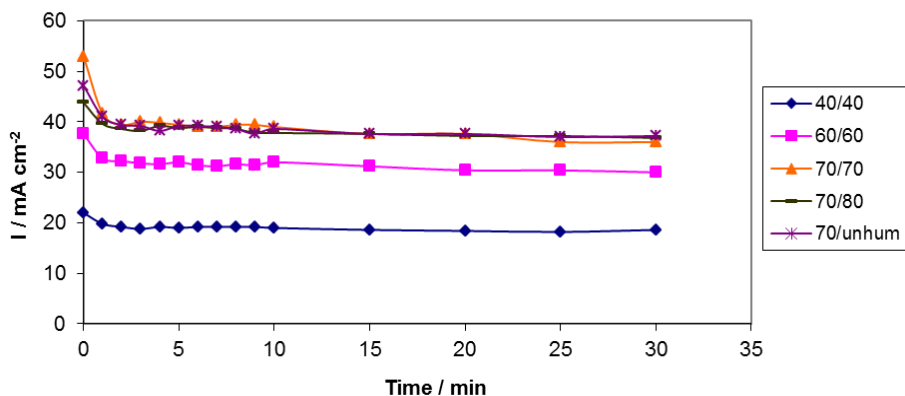


Fig. 5 The current density decay of the single cell in Fig. 4 at 0.4 V

elevated temperature. The current density declined at 40 °C was at 6.06% but became 13.46% at 70 °C. The high decaying rate may result from several causes. First, the faster reaction rate at higher temperatures resulted in higher turnover frequency of glycerol electrooxidation, as a consequence, produced higher amount of poisonous products. Second, glycerol electrooxidation was a complex reaction involves a number of steps via parallel pathways (Yongprapat *et al.* 2012). The change in temperature can cause a change in a product distribution.

The humidification condition was not a problem in the study condition. Long period of unhumidification did not affect the cell performance. The current density decay in unhumidification condition was lower than that of the humidification one. Normally, an absence of humidity at the cathode should promote the transport of ions from the anode to the cathode. Despite a non-selective porous membrane, along with the water and hydroxide, the glycerol was also transferred. The lower current decay rate may point out a low seriousness of the glycerol crossover from anode to cathode. However, this was a subject for further study.

### 3.3 Comparison between Au/C and PtRu/C catalyst

This section compares the performance of the single cell using Au/C and PtRu/C as anode catalysts. All the single cells were constructed in the same way as previously described. The cell performance was compared at 70 °C of cell temperature and humidification temperature. The glycerol concentration remains at 1 M but the KOH concentration was varied at 2 M and 4 M.

Fig. 6 shows the polarization curves and power density curves of the single cell using Au/C and PtRu/C catalysts at both concentrations of KOH. The results indicated a superior activity of the Au/C catalyst for glycerol electrooxidation. Performance of the single cell with Au/C was higher than that with PtRu/C at the same condition. The maximum current densities of the single cell with PtRu/C were 33.2 and 37.1 mA cm<sup>-2</sup> at 2 and 4 M KOH, respectively, while those of the Au/C single cell was at 38.9 and 46.4 mA cm<sup>-2</sup> for the same condition. This was because the Au-based catalyst was much more active for glycerol electrooxidation in alkaline than PtRu/C (Yongprapat *et al.* 2012).

Increasing KOH concentration improves the activity of both single cells. The increasing rate was much higher for Au/C than for PtRu/C at 19% and 11%, respectively. The addition of

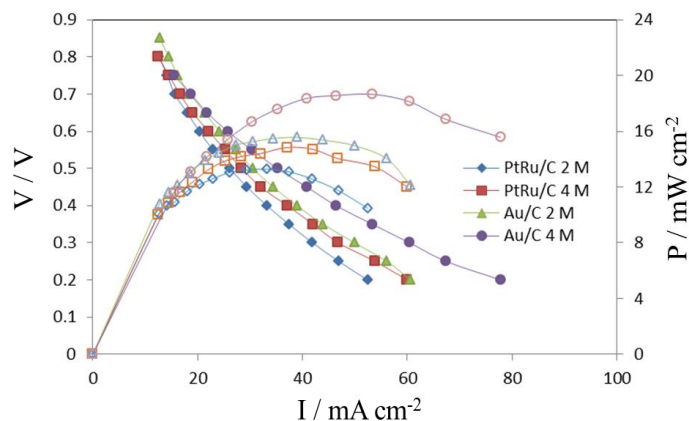


Fig. 6 Polarization curves and power density curves of the single cell using Au/C and PtRu/C as anode catalysts using 1 M glycerol with 2 or 4 M KOH mixed fuel at 70°C

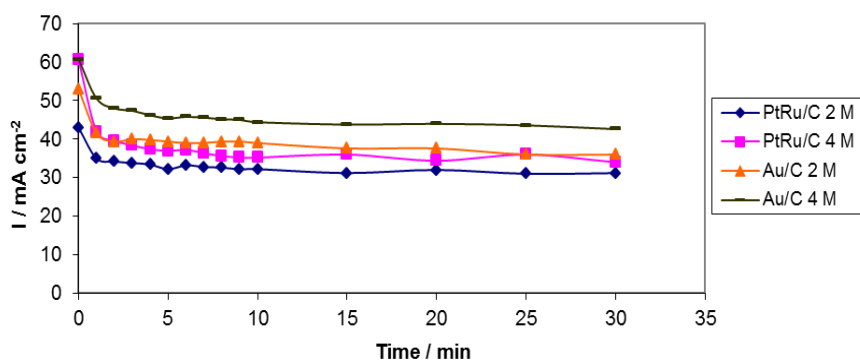


Fig. 7 The current density decay of the single cell in Fig. 6 at 0.4 V

hydroxide solution provides different benefits to Au- and Pt-based catalysts. For Au-based catalyst, the rate determining step of glycerol electrooxidation was the adsorption of alcohol on Au surface. This process was either induced by the pre-adsorbed hydroxide on Au surface (Betowska-brzezinska *et al.* 1997) or the adsorption of deprotonated alcohol (Kwon *et al.* 2011). Increasing KOH concentration promoted both mechanisms and the overall reaction rate. For Pt-based catalyst, the rate determining step was the removal of the poisonous species from the catalyst surface. Hydroxyl on Pt surface was used to remove the poisonous species via a bifunctional mechanism (Watanabe 2003).

Fig. 7 shows the current density decay curves at 0.4 V for the single cell having the performance shown in Fig. 6. The current density trend was similar to that of the polarization curves. The single cell with Au/C yields the highest current density at 50.6 mA cm<sup>-2</sup>, as shown in Table 3. The decay of all the cells was higher than 10%. The decay in 2 M KOH of PtRu/C was slightly lower than that of Au/C. The decay of current density was higher with increasing KOH concentration. This resulted from a better activity of the catalyst. As KOH concentration was increased, the deactivation of the single cell with PtRu/C was almost one fold higher, while that of Au/C slightly increased. As a result, the single cell using Au/C became more stable.



Table 3 Current density in mA cm<sup>-2</sup> unit and the decay rate from the 1<sup>st</sup> minute and 30<sup>th</sup> minute of the single cell in Fig. 6 at 0.4 V

Catalyst	KOH (M)	I at 1 <sup>st</sup> min	I at 30 <sup>th</sup> min	Current decay rate (%)
PtRu/C	2	35.0	31.2	10.86
	4	42.0	34.0	19.05
Au/C	2	41.6	36.0	13.46
	4	50.6	42.6	15.81

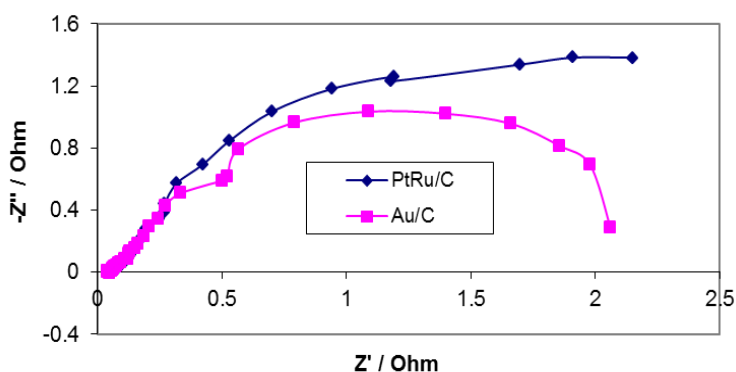


Fig. 8 Impedance spectra of the single cells using Au/C and PtRu/C at a constant current of 50 mA. The cell was operated at 70 °C, anode feed: 1 ml min<sup>-1</sup> of 1 M glycerol and 2 M KOH, cathode feed: O<sub>2</sub> at 46 ml min<sup>-1</sup>

The impedance measurement was used to measure the activation loss of the single cell. The impedance spectra of the single cell using Au/C and PtRu/C at a constant current of 50 mA are shown in Fig. 8. The activation loss can be observed from the intersection of the higher frequency arc on the real axis. The intersection of the single cell with Au/C was around 2 Ohm. For the single cell with PtRu/C, the intersection should be by far higher than 2 Ohm. This indicates a much lower activation loss of Au/C catalyst over PtRu/C.

## 5. Conclusions

The electrocharacteristic of the single cell using microporous polypropylene Celgard 3401 for direct glycerol alkaline fuel cell was evaluated. In comparison with Nafion 112, the single cell with Celgard 3401 membrane provide around 32% higher in current density and power density. This resulted from the lower ionic resistance of Celgard 3401 than Nafion 112.

The performance of Au/C prepared by PVA protection method for direct glycerol alkaline fuel cells using microporous polymeric membrane was evaluated in comparison with PtRu/C. The performance of both single cells greatly depended on the cell temperature. The current density was increased around one fold when the cell temperature was increased from 40 to 70 °C. However, the cell performance did not depend on the humidification condition at the cathode. This pointed out the sufficient water transferred from the anode to the cathode.

The single cell using Au/C showed better performance than that of PtRu/C for every condition.

The current densities at 0.4 V for the single cell operated at 70 °C using Au/C and PtRu/C were 38.9 and 33.2 mA cm<sup>-2</sup> with the maximum power density at 15.56 and 13.28 mW cm<sup>-2</sup>, respectively. The impedance spectra indicated the lower activation loss of Au/C over PtRu/C. The performance was improved at higher KOH concentration. The current density of the single cell using Au/C was increased to 46.4 mA cm<sup>-2</sup> with the maximum power density of 18.56 mW cm<sup>-2</sup>.

The results showed that the porous membrane was capable for the alkaline direct alcohol fuel cell. However, the cathode catalyst in this study was active for glycerol electrooxidation. Thus, it was suffered from the glycerol crossover. The type of catalyst at the cathode and the fuel cell structure will be the subjects for our further study.

## Acknowledgements

This work was financially supported by the Joint Graduate School of Energy and Environment (JGSEE) and the National Nanotechnology Center of Thailand (NANOTEC). The first author would like to thank the Royal Golden Jubilee (RGJ) program of the Thailand Research Fund (TRF) and JGSEE for the jointed academic scholarship.

## References

- An, L. Zhao, T.S., Li, Y. and Wu, Q. (2012), "Charge carriers in alkaline direct oxidation fuel cells", *Energy Environ. Sci.*, **5**, 7536-7538.
- Arges, C.G., Parrondo, J., Johnson, G., Nadham, A. and Ramani, V. (2012), "Assessing the influence of different cation chemistries on ionic conductivity and alkaline stability of anion exchange membranes", *J. Mater. Chem.*, **22**, 3733-3744.
- Arges, C.G. and Ramani, V. (2013), "Investigation of cation degradation in anion exchange membranes using multi-dimensional NMR spectroscopy", *J. Electrochem. Soc.*, **160** (9), F1006-F1021.
- Betowska-brzezinska, M., Uczak, T. and Holze, R. (1997), "Electrocatalytic oxidation of mono- and polyhydric alcohols on gold and platinum", *J. Appl. Electrochem.*, **27**(9), 999-1011.
- Blizanac, B.B., Ross, P.N. and Markovic, N.M. (2007), "Oxygen electroreduction on Ag(111): The pH effect", *Electrochim. Acta.*, **52**(6), 2264-2271.
- Bunazawa, H. and Yamazaki, Y. (2009), "Ultrasonic synthesis and evaluation of non-platinum catalysts for alkaline direct methanol fuel cells", *J. Power Sour.*, **190**(2), 210-215.
- Change, S., Ho, Y. and Weaver, M.J. (1991), "Applications of real-time FTIR spectroscopy to the elucidation of complex electroorganic pathways: Electrooxidation of ethylene glycol on gold, platinum and nickel in alkaline solution", *J. Am. Chem. Soc.*, **113**, 9506-9513.
- Demarconnay, L., Contaudeau, C. and L  ger, J.M. (2004), "Electroreduction of dioxygen (ORR) in alkaline medium on Ag/C and Pt/c nanostructured catalysts-effect of the presence of methanol", *Electrochim. Acta.*, **49**(25), 4513-4521.
- Kwon, Y., Lai, S.C.S., Rodriquez, P. and Koper, M.T.M. (2011), "Electrocatalytic oxidation of alcohols on gold in alkaline media: Base or gold catalysis?", *J. Am. Chem. Soc.*, **133**(18), 6914-6917.
- Lima, F.H.B., Calegaro, M.L. and Ticianelli, E.A. (2006), "Investigations of the catalytic properties of manganese oxides for the oxygen reduction reaction in alkaline media", *J. Electroanal. Chem.*, **590**(2), 152-160.
- Maurya, S., Shin, S.H., Kim, M.K., Yun, S.H. and Moon, S.H. (2013), "Stability of composite anion exchange membranes with various functional groups and their performance for energy conversion", *J. Membr. Sci.*, **443**, 28-35.
- Nunez, S.A. and Hickner, M.A. (2013), "Quantitative <sup>1</sup>H NMR analysis of chemical stabilities in anion

- exchange membrane”, *Macro. Lett. - ACS.*, **2**, 49-52.
- Padayachee, D., Golovko, V. and Marshall, A.T. (2013), “The effect of MnO<sub>2</sub> loading on the glycerol electrooxidation activity of Au/MnO<sub>2</sub>/C catalysts”, *Electrochim. Acta*, **98**, 208-217.
- Pattabiraman, R. (1997), “Electrochemical investigations on carbon supported palladium catalysts”, *Appl. Catal. A.Gen.*, **153**(1-2), 9-20.
- Shen, P.K. and Xu, C. (2006), “Alcohol oxidation on nanocrystalline oxide Pd/C promoted electrocatalysts”, *Electrochem. Comm.*, **8**(1), 184-188.
- Watanabe, M. (2003), *Design of electrocatalysts for fuel cells in: Wieckowski, A., Savinova, E.R., Vayenas, C.G. eds., Catalysis and electrocatalysis at nanoparticle surfaces*, Marcel Dekker, Inc. America.
- Xin, L., Zhange, Z., Qi, J., Chadderdon, D. and Li, W. (2012), “Electrocatalytic oxidation of ethylene glycol(EG) onsupported Pt and Au catalysts in alkaline media: reaction pathway investigation in three-electrode cell and fuel cell reactors”, *Appl. Catal. B.*, **125**, 85-94.
- Yang, Y., Zhou, Y. and Cha, C. (1995), “Electrochemical reduction of oxygen on small palladium particles supported on carbon in alkaline solution”, *Electrochim. Acta*, **40**(16), 2579-2586.
- Yongprapat, S., Therdthianwong, A. and Therdthainwong, S. (2012), “Au/C catalyst prepared by polyvinyl alcohol protection method for direct alcohol alkaline exchange membrane fuel cell application”, *J. Appl. Electrochem.*, **42**(7), 483-490.
- Zhange, J.H., Liang, Y.J., Li, N., Li, Z.Y., Xu, C.W. and Jiang, S.P. (2012), “Remarkable activity of glycerol electrooxidation on gold in alkaline medium”, *Electrochim. Acta.*, **59**, 156-159.
- Zhange, Z., Xin, L. and Li, W. (2012), “Supported gold nanoparticles as anode catalyst for anion-exchange membrane-direct glycerol fuel cell (AEM-DGFC)”, *Int. J. Hydrogen Energ.*, **37**(11), 9393-9401.